数理解析研究所講究録
第520巻 1984年 105-134

Triplet Distribution Function of the Fluid with the Square Well Potential

東北大工 佐藤広也 (Hiroya Satoh)
東北大工 田中 実 (Minoru Tanaka)
東北大工 桂 重俊 (Shigetoshi Katsura)

The triplet distribution function of the fluid with the square well potential is calculated at the leading order of ρ by two methods: one is the method of generalized Fourier tramsform combined with the addition theorem of Bessel functions, and another is the geometrical method. The results are compared with those computed by the Monte Carlo and the molecular dynamics simulations. Higher order calculation by our scheme seems to be promissing.

1. Introduction

The generic probability density that each of the distinct volume elements $d\mathbf{r}_1, d\mathbf{r}_2, \ldots, d\mathbf{r}_q$ situated at the positions $\mathbf{r}_1, \mathbf{r}_2, \ldots, \mathbf{r}_q$ is occupied simultaneously by each of q molecules of a uniform fluid, is denoted by $n^{(q)}(\mathbf{r}_1, \mathbf{r}_2, \ldots, \mathbf{r}_q)$: $n^{(1)}=\rho$ is the number density, $n^{(2)}(\mathbf{r}_1, \mathbf{r}_2)$ is the pair distribution function, and $n^{(3)}(\mathbf{r}_1, \mathbf{r}_2, \mathbf{r}_3)$ is the triplet distribution function. In a simple liquid at equilibrium of given temperature and density, the molecular distribution function $n^{(q)}(q \geq 2)$ is a function of the relative positions $\mathbf{r}_{ij}$ and determined by the intermolecular potential $\phi(r)$. They can be measured by the X-ray or neutron diffraction, and calculated by the Monte Carlo [1] and the molecular dynamics [2] simulations.

The pair and triplet distribution functions, $n^{(2)}(\mathbf{r}_1, \mathbf{r}_2) \equiv \rho^2 g(r_{12})$ and $n^{(3)}(\mathbf{r}_1, \mathbf{r}_2, \mathbf{r}_3) \equiv \rho^3 g^{(3)}(r_{12}, r_{23}, r_{31})$, are expressed by [3,4]

$$g(r_{12}) = \exp\left[-\beta\phi(r_{12}) + \sum_{\ell=1}^{\infty} \frac{\rho^{\ell}}{\ell!} \delta_{\ell}^{(2)}(r_{12})\right], \tag{1.1}$$

$$g^{(3)}(r_{12}, r_{23}, r_{31}) = g_2(r_{12}) g_2(r_{23}) g_2(r_{31}) \times \exp\left[\sum_{\ell=1}^{\infty} \frac{\rho^{\ell}}{\ell!} \delta_{\ell}^{(3)}(r_{12}, r_{23}, r_{31})\right], \tag{1.2}$$

where

$$\delta_1^{(2)}(r_{12}) = \int f_{12} f_{31} d\mathbf{r}_3 = \quad , \tag{1.3}$$

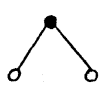

$$\delta_2^{(2)}(r_{12}) = \int (2 f_{13} f_{34} f_{42} + 4 f_{13} f_{34} f_{42} f_{14} + f_{13} f_{34} f_{42} f_{14} f_{23}) d\mathbf{r}_3 d\mathbf{r}_4$$

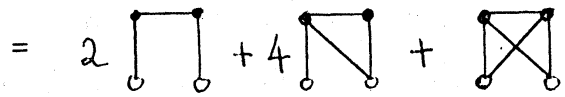

(1.4)

$$\delta_1^{(3)}(r_{12},r_{23},r_{31}) = \int f_{14}f_{24}f_{34}dr_4 =$$

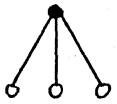

, (1.5)

$$\delta_2^{(3)}(r_{12},r_{23},r_{31}) = 2\{$$

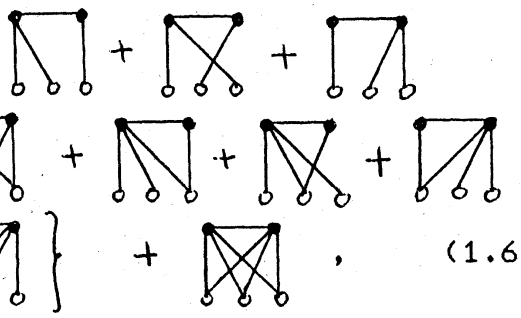

$$\}$$

, (1.6)

and

$$f_{ij} = f(r_{ij}) = \exp[-\beta\phi(|\mathbf{r}_i - \mathbf{r}_j|)] - 1.$$

We call the exponential factor in (1.2) simply as the triplet correlation function in the following. The zeroth approximation of (1.2) where the factor exp[ ] is replaced by 1, is the superposition approximation, and it gives the virial coefficients up to the third exactly. The fourth coefficient is given exactly by taking account of the leading term in the triplet correlation function, i.e., the first order term $\delta_1^{(3)}$.

For the hard sphere fluids, $\delta_1^{(2)}$ and $\delta_2^{(2)}$ were obtained by Nijboer and Van Hove [5]. For the fluids with the square well potential, $\delta_1^{(2)}$ and the first two terms of $\delta_2^{(2)}$ were obtained by McQuarrie [6] and the last by Katsura and Nishihara [7]. $\delta_1^{(3)}$ for the hard sphere fluids was discussed by Abe [8], Rowlinson [9], and Powell [10].

In a realistic simple fluids, the attraction plays important role which is irrelevant in the hard sphere system. Since the overall properties of fluids do not depend on the details of the shape of potential, we here consider the square

well potential instead of the Lennard-Jones one. The parameters of the square well potential are determined in such a way that the Boyle temperature and the temperature gradient of the second virial coefficient at the Boyle temperature coincide with those calculated for the Lennard-Jones system [11], and the triple and the critical temperatures of the latter correspond to $kT_{tr}/\varepsilon \simeq 1.52$ and $kT_c/\varepsilon \simeq 2.83$ in our model.

For the calculations of the molecular distribution function and virial coeffcients, we must evaluate integrals of the type

$$\int \Pi f_{ij} \Pi' d\mathbf{r}_k,$$

for which in a case of cyclic indices as

$$\int f_{12} f_{23} f_{34} \cdots f_{k1} d\mathbf{r}_1 d\mathbf{r}_2 \cdots d\mathbf{r}_k,$$

the method of Fourier transform is effective. The Fourier transform method has been generalized by Katsura and applied to evaluate complex clusters in the calculations for the fourth [12] and the fifth [13,14] virial coefficients, and also to calculate the distribution functions [7].

In this paper, the leading term of the triple correlation function, $\delta_1^{(3)}(r_{12}, r_{23}, r_{31})$ for the fiuid with the square well potential is evaluated and discussed. We discuss the analytical method in the section 2 and the geometrical one in the section 3. The last section 4 is devoted to the discussion of the numerical results and the comparison with the computer simulations.

2. Analytical method

Integrals involved in the expressions of $\delta_{\ell}^{(3)}$, can be calculated by the combination of the Fourier transform and the addition theorem of Bessel functions. [7,12,13,14]. For the square well potential, f(r) is given by

$$f(r) = \begin{cases} 1 & (0 < r < 1), \\ f \equiv e^{\beta\varepsilon}-1 & (1 < r < s), \\ 0 & (s < r). \end{cases} \qquad (2.1)$$

The Fourier transform of f(r), $\gamma(t)$ is given by

$$\gamma(\mathbf{t})=\gamma(t)=(2\pi)^{-3/2}\int f(r)\exp(-i\mathbf{t}.\mathbf{r})d\mathbf{r} \qquad (2.2)$$

$$=(1+f)\gamma_0(t)-fs^3\gamma_0(st), \qquad (2.2')$$

where $\gamma_0(t)$ is the $\gamma(t)$ with the hard sphere potential:

$$\gamma_0(t)=(2/\pi)^{1/2}\left(\frac{\cos t}{t^2}-\frac{\sin t}{t^3}\right)\equiv -\frac{J_{3/2}(t)}{t^{3/2}}. \qquad (2.3)$$

Substituting (2.2) into (1.5), we have

$$\delta_1^{(3)}(\mathbf{r}_1,\mathbf{r}_2,\mathbf{r}_3)=(2\pi)^{-3/2}\int\delta(\mathbf{t}_1+\mathbf{t}_2+\mathbf{t}_3)\gamma(\mathbf{t}_1)\gamma(\mathbf{t}_2)\gamma(\mathbf{t}_3)$$

$$\times\exp[i(\mathbf{t}_1.\mathbf{r}_1+\mathbf{t}_2.\mathbf{r}_2+\mathbf{t}_3.\mathbf{r}_3)]d\mathbf{t}_1d\mathbf{t}_2d\mathbf{t}_3$$

$$=\Sigma_{\lambda\mu\nu}(1+f)^{n_1}(-fs^3)^{n_2}I_{\lambda\mu\nu}(\mathbf{r}_1,\mathbf{r}_2), \qquad (2.4)$$

where

$$I_{\lambda\mu\nu}(\mathbf{r}_1,\mathbf{r}_2)=(2\pi)^{-3/2}\int\gamma_0(\lambda t_1)\gamma_0(\mu t_2)\gamma_0(\nu(t_1+t_2))$$

$$\times\exp[i(\mathbf{t}_1\cdot\mathbf{r}_1+\mathbf{t}_2\cdot\mathbf{r}_2)]dt_1dt_2. \qquad (2.5)$$

The symbol $\Sigma_{\lambda\mu\nu}$ means the summation over 8 cases where each of the parameters λ, μ, ν takes the value 1 or s, and $n_1(n_2)$ is the number of those equal to 1(s) for each of $I_{\lambda\mu\nu}$. Let $t_2=-t_2'$ and we decompose $\gamma(\nu(t_1-t_2'))$ with use of the addition theorem (A.1) and substitute (A.2) into (2.5), we have

$$I_{\lambda\mu\nu}(\mathbf{r}_1,\mathbf{r}_2)=-\Sigma_{n=0}^{\infty}\Sigma_{p=0}^{\infty}\Sigma_{q=0}^{\infty}\left(\frac{3}{2}+n\right)\left(\frac{1}{2}+p\right)\left(\frac{1}{2}+q\right)i^p(-i)^q(\lambda\mu)^{-3/2}$$

$$\times\nu^{-3}W_{3/2,3/2+n,1/2+p}{}^{3/2}(\lambda,\nu,r_1)\;W_{3/2,3/2+n,1/2+q}{}^{3/2}(\mu,\nu,r_2)$$

$$\times\int C_n^{3/2}(\cos\psi_{t1-t2'})P_p(\cos\psi_{t1-r1})P_q(\cos\psi_{t2'-r2})d\Omega_{t1}d\Omega_{t2'},$$

$$(2.6)$$

where $\psi_{t1-t2'}$ and $\psi_{t2'-r2}$ are the included angles between $\mathbf{t}_1$ and $\mathbf{t}_2'$, and $\mathbf{t}_2'$ and $\mathbf{r}_1$, respectively, $d\Omega_t=\sin\theta_t d\theta_t d\phi_t$, and $C_n^{3/2}(\cos\psi)$ is the Gegenbauer polynomial which is expressed by Legendre functions as in (A.3). With use of (A.4), the integrals over the solid angles lead to the result as

$$\int C_n^{3/2}(\cos\psi_{t1-t2'})P_p(\cos\psi_{t1-r1})P_q(\cos\psi_{t2'-r2})d\Omega_{t1}d\Omega_{t2'}$$

$$=\begin{cases}(4\pi)^2\delta_{pq}\dfrac{1}{2p+1}P_p(\cos\psi_{r1-r2}), & n\geq p\geq 0,\ n+p \text{ even},\\ 0, & \text{otherwise}.\end{cases}$$

$$(2.7)$$

Hence we have

$$I_{\lambda\mu\nu}(\mathbf{r}_1,\mathbf{r}_2)=-\frac{1}{2}(4\pi)^2(\lambda\mu)^{-3/2}\nu^{-3}(r_1r_2)^{-1/2}$$
$$\times \Sigma_{n=0}^{\infty} \quad \Sigma'^{n}_{p=0} \quad (\tfrac{3}{2}+n)(\tfrac{1}{2}+p)$$
$$\times W_{3/2,3/2+n,1/2+p}^{3/2}(\lambda,\nu,r_1)\, W_{3/2,3/2+n,1/2+p}^{3/2}(\mu,\nu,r_2)$$
$$\times P_p(\cos\psi_{\mathbf{r}1-\mathbf{r}2}), \qquad (2.8)$$

where the summation Σ' for p runs only over integers with the same parity with n, and

$$W_{3/2,3/2+n,1/2+p}^{3/2}(a,b,c)$$
$$\equiv\int_0^{\infty}J_{3/2}(at)J_{3/2+n}(bt)J_{1/2+p}(ct)t^{-3/2}dt. \qquad (2.9)$$

Substituting (A.5) into (2.9) and let $s\equiv it$, we have

$$W_{3/2,3/2+n,1/2+p}^{3/2}(a,b,c)=i(-1)^{(n+p)/2}(2\pi)^{-3/2}(abc)^{-1/2}$$
$$\times \Sigma_{m=0}^{1} \Sigma_{\ell=0}^{n+1} \Sigma_{u=0}^{p} \frac{(1+m)!}{m!(1-m)!}\frac{(n+1+\ell)!}{\ell!(n+1-\ell)!}\frac{(p+u)!}{u!(p-u)!}$$
$$\times a^{-m}\, b^{-\ell}\, c^{-u}\, P\int_{-i\infty}^{i\infty}ds \;\; s^{-3}\,(2s)^{-(\ell+m+u)}$$
$$\times[(-1)^{m+\ell+u}\, e^{s(a+b+c)} +(-1)^{p+m+\ell+1}\, e^{s(a+b-c)}$$
$$+(-1)^{n+m+u}\, e^{s(a-b+c)} +(-1)^{n+m+p+1}\, e^{s(a-b-c)}].$$

(2.10)

The principal integral in (2.10) is obtained by the residue theorem which leads to the formula (A.6), and we have

$$W_{3/2,3/2+n,1/2+p}^{3/2}(a,b,c)=-(-1)^{(n+p)/2}\pi(2\pi)^{-3/2}$$

$$\times (abc)^{-1/2} \sum_{m=0}^{1} \sum_{\ell=0}^{n+1} \sum_{u=0}^{p} a^{-m} b^{-\ell} c^{-u} 2^{-(\ell+m+u)}$$

$$\times \frac{(1+m)!}{m!(1-m)!} \frac{(n+1+\ell)!}{\ell!(n+1-\ell)!} \frac{(p+u)!}{u!(p-u)!} \frac{1}{(2+m+\ell+u)!}$$

$$\times [\ (-1)^{m+\ell+u} \mathrm{sgn}(a+b+c)\ (a+b+c)^{2+m+\ell+u}$$

$$+(-1)^{p+m+\ell+1} \mathrm{sgn}(a+b-c)\ (a+b-c)^{2+m+\ell+u}$$

$$+(-1)^{n+m+u} \mathrm{sgn}(a-b+c)\ (a-b+c)^{2+m+\ell+u}$$

$$+(-1)^{n+P+m+1} \mathrm{sgn}(a-b-c)\ (a-b-c)^{2+m+\ell+u}\ ].$$

(2.11)

The expression (2.11) is evaluated up to n=8 by use of the formula-manipulation computer language REDUCE [15]. The leading term $\delta_1^{(3)}(a, b, c)$ is calculated in the case of s=2 by (2.4) with (2.8) and (2.11),and will be discussed in the section 4.

3. Geometrical method

The leading term in the triplet correlation function, $\delta_1^{(3)}$ for the hard sphere fluid has been calculated by the simple geometrical argument [8,9,10]. In this section, we show that it can be calculated also for the square well potential by a purely geometrical consideration. Let us consider the three spheres at A, B and C with the radii r_a, r_b and r_c respectively. Let a, b and c be the three sides of the triangle formed by A, B and C, and $V(a,b,c;r_a,r_b,r_c)$ (≥ 0) the volume of the common intersection of these three spheres. Then $\delta_1^{(3)}(a, b, c)$ is given by

$$\delta_1^{(3)}(a,\ b,\ c)$$

$$= -(1+f)^3V(a,b,c;1,1,1)$$

$$+ (1+f)^2f[V(a,b,c;1,1,s)+V(a,b,c;1,s,1)+V(a,b,c;s,1,1)]$$

$$- (1+f)f^2[V(a,b,c;1,s,s)+V(a,b,c;s,1,s)+V(a,b,c;s,s,1)]$$

$$+ f^3V(a,b,c;s,s,s). \qquad (3.1)$$

The geometrical situations are classified in several cases according to the values of r_a, r_b, r_c, a, b, c. In the following interpretation the indices a, b and c should be changed in cyclic way as a → b → c → a if necessary.

When three intersecting circles of the spheres A, B, C have common two points P and P′, $V(a,b,c;r_a,r_b,r_c)$ is given by [10]

$$V(a,b,c;r_a,r_b,r_c) = 2V_t - 2(Z_a+Z_b+Z_c) + 2(Y_a+Y_b+Y_c),$$

where V_t is the volume of the tetrahedron PABC, Z_a is the volume of the sphere A enclosed by the solid angle at the point A of the tetrahedron PABC, and Y_a is the volume of the common part of spheres B and C enclosed by the two faces of the tetrahedron PABC which meet in BC (see Fig.1). These quantities are given as follows;

$$V_t=\sqrt{Q}/12, \qquad (3.2)$$

$$Z_a\equiv r_a^3[\tan^{-1}(r_a\sqrt{Q}/4E_{ra})+\tan^{-1}(b\sqrt{Q}/4E_b)+\tan^{-1}(c\sqrt{Q}/4E_c)-\pi]/3, \qquad (3.3)$$

$$Y_a\equiv Y_{a0}\tan^{-1}(a\sqrt{Q}/4E_a)/2\pi, \qquad (3.4)$$

where

$$Q \equiv (b^2+c^2-a^2)(a^2r_a^2+r_b^2r_c^2)+(a^2-b^2+c^2)(b^2r_b^2+r_c^2r_a^2) \quad (3.5)$$

$$E_a \equiv [(a^2+b^2-c^2)r_b^2+(a^2-b^2+c^2)r_c^2+(b^2+c^2-a^2-2r_a^2)a^2]/8 \quad (3.6)$$

$$E_{ra} \equiv [(r_a^2+b^2-r_c^2)r_b^2+(r_a^2-b^2+r_c^2)c^2+(b^2+r_c^2-r_a^2-2a^2)r_a^2]/8 \quad (3.7)$$

$$Y_{a0} \equiv (\pi/3)[2r_b^3-3r_b^2(a^2+r_b^2-r_c^2)/2a+(a^2+r_b^2-r_c^2)^3/8a^3. \quad (3.8)$$

Here, Y_{a0} is the volume of the common part of the spheres B and C. In the expressions of Y_a and Z_a, $\tan^{-1}(a\sqrt{Q}/4E_a)$ is the angle between the planes ABC and PBC. The branch of $\tan^{-1}x$ is taken in $0 < \tan^{-1}x < \pi$.

Let R be the point which lies on the intersecting circle of the spheres B and C and is most distant from A, and F_a be the distance between A and R (Fig.2). Then

$$F_a^2 \equiv [(r_b^2-r_c^2+b^2-c^2)^2+\{[4b^2c^2-(b^2+c^2-a^2)^2]^{1/2} + [4a^2r_b^2-(a^2+r_b^2-r_c^2)^2]^{1/2}\}^2]/4a^2. \quad (3.9)$$

When three intersecting circles of the spheres A, B, C have no common points of intersections $V(a,b,c;r_a,r_b,r_c)$ is classified by the indicators I_a and L_a.

$$I_a \equiv [\mathrm{sgn}(|r_b-r_c|-a)+1]/2, \quad (3.10)$$

$$L_a \equiv [\mathrm{sgn}(F_a^2-r_a^2)+1]/2. \quad (3.11)$$

The expression of $V(a,b,c;r_a,r_b,r_c)$ is classified in term of the above notations in Table 1 and Fig.3. When $r_a=r_b=r_c=1$, our results agree whith those given by Powell [10].

4. Discussion

The analytical method to calculate $\delta_1^{(3)}(r_{12},r_{23},r_{31})$ leads to the expression (2.4) where $I_{\lambda\mu\nu}(\mathbf{r}_1,\mathbf{r}_2)$ is given as the infinite series (2.8). Each term in (2.8) is given in a compact form as in (2.11) which is easily calculated algebraically. The analytical method may be easily generalized to calculate the higher order terms $\delta_\ell^{(3)}$($\ell \geq 2$). The geometrical method shown in the section 3, on the other hand, leads to the closed expression (3.1) and can be calculated in a straightforward way accoding to the classification shown in Table 1.

In this section we first show the numerical results of $\delta_1^{(3)}(r_{12},r_{23},r_{31})$ by our two methods for several configurations of three particles, and secondly compare them with the results obtained by the Monte Carlo and the molecular dynamics simulations as is stated in the introduction. We take the square well potential parameter s in (2.1) arbitrarily as s = 2 for the calculations throughout the following.

In Fig.4, the convergence of the series (2.8) of the analytical method is shown for the case of equilateral triplets, i.e., $\delta_1^{(3)}(r,r,r)$ with $kT/\varepsilon = 2.0$. Comparing with the exact result by the geometrical method, we have found that the series (2.8) can be truncated at n = 8 to give almost exact results as shown in Fig.4. This is true also for $\delta_1^{(3)}(r_{12},r_{23},r_{31})$ of more general configurations of the triplets, and seems to promise a success of our analytical method discussed in the section 2 to be applied to the higher order terms $\delta_\ell^{(3)}$($\ell \geq 2$).

In the following the numerical analysis of

$\delta_1^{(3)}(r_{12},r_{23},r_{31})$ is shown for arbitrarily fixed values of r_{12} and kT/ε with varying r_{23} and r_{31} as the contour lines on the first quadrant of the XY plane where the particles 1 and 2 are fixed at $(0,r_{12}/2)$ and $(0,-r_{12}/2)$ respectively as shown in Fig.5. In the following figures the dashed circle around the cross on the Y axis shows the diameter of the hard sphere repulsion around the particle, and inside the circle $g^{(3)}(r_{12},r_{23},r_{31})$ vanishes identically. As is shown in the rows [1] and [5] of Table 1, the leading term $\delta_1^{(3)}(r_{12},r_{23},r_{31})$ vanishes outside the outmost dashed curve in each of Figs.6 and 7.

In Fig.6 we show $\delta_1^{(3)}(r_{12},r_{23},r_{31})$ at $kT/\varepsilon = 1.6$ for $r_{12} =$ 1.0, 1.6, 2.6 and 3.0, and at $kT/\varepsilon = 5.0$ in Fig.7 for $r_{12} = 1.0$, 1.6, 2.6 and 3.0. With these results and further analysis at intermediate temperatures, the overall features of variation of $\delta_1^{(3)}(r_{12},r_{23},r_{31})$ with the configuration of the triplet can be summarized as shown in Fig.8. At lower temperature ($kT/\varepsilon \lesssim 2$) for smaller values of r_{12}($r_{12} \lesssim 2.5$), local minimum and maximum appear on the X axis, i.e., with isosceles configurations of the triplet. While a negative region appears near the Y axis corner, i.e., with almost linear configurations (Fig.8(a)). As r_{12} increases ($2.5 \lesssim r_{12} \lesssim 3.0$), the minimum point is shifted to the oringin, i.e., to the midpoint between the particles 1 and 2 while the maximum changes into a saddle point (Fig.8(b)). And for $r_{12} \gtrsim 3.0$ the negative region near the Y axis corner vanishes (Fig.8(c)).

At higher temperature ($kT/\varepsilon \simeq 5$) the variation of $\delta_1^{(3)}$ with r_{12} is similar to those in Fig.8 although the difference between

maximum and minimum becomes smaller. It is interesting to see some sort of correspondence between Figs.6 and 7: the features of contour lines in (a), (b) and (c) of Fig.6 are roughly similar to those in (b), (c) and (d) of Fig.7, respectively. In the limit of $T \to \infty$ $\delta_1^{(3)}$ becomes negative inside the nonzero region and the contour lines seems somewhat like a shallow elliptic bowl.

The variation of $\delta_1^{(3)}(r_{12},r_{23},r_{31})$ with the configuration of the triplet as is shown in Fig.6, 7 and 8 can be considered to show a qualitative feature of the leading term in the triplet correlation function in a classical simple liquid with an ordinary interaction potential such as the Lennard-Jones one:

$$\phi(r) = 4u[(\sigma/r)^{12} - (\sigma/r)^{6}]. \qquad (4.1)$$

If we assume a law of corresponding states at the Boyle temperature at a given number density ρ, the parameters u and σ in (4.1) can be related to ε and the radius (= 1) in (2.1) as

$$kT/u = 0.459kT/\varepsilon, \qquad \rho\sigma^3 = 1.318\rho, \qquad (4.2)$$

and therefore the triple and the critical tempertures of the Lennard-Jones liquid correspond to $kT_{tr}/\varepsilon \simeq 1.52$ and $kT_c/\varepsilon \simeq 2.83$ in our model. The results shown in Fig.6 correspond to a state near T_{tr} and those in Fig.7 well above T_c.

Reveché and Mountain [1] reported elaborate calculations of the triplet crrelation function of the Lennared-Jones liquid by the Monte Carlo simulation for several states avove the triple point. Among their results, Fig.3(b) of [1] at $\rho\sigma^3 = 0.850$ and $kT/u = 0.719$ with $r_{12} = 1.525\sigma$ can be assumed to correspond to a state at $kT/\varepsilon = 1.57$ with $r_{12} = 1.67$ in our model. We show the

logarithm of the result by Raveché and Mountain in Fig.9 which should be compared with Fig.6(b). The overall feature of contour lines in Fig.9 is qualitatively simlar to those in Fig.6(b) except their heights and the appearance of extra maxima. The difference reflects the ignorance of the higher order terms $\delta_{\ell}^{(3)}(\ell \geq 2)$ in Fig.6(b). We have done the molecular dynamics simulation of the Lennard-Jones system (argon) near T_{tr} and calculated $g^{(3)}(r_{12},r_{23},r_{31})$ for several configurations of the triplet. With the results for the isosceles triplets, i.e., $g^{(3)}(s,r,r)$ (s,fixed), we compare the change of $\delta_1^{(3)}(r_{12},r_{23},r_{31})$ along the x axis in Fig.10. The general agreement is again obtained except at smaller r.

We consider that our two methods and the results as shown in Fig.6, 7 and 8 are useful to show a general feature of the leading term in the triplet correlation function, i.e., for $g^{(3)}(r_{12},r_{23},r_{31})/[g(r_{12})g(r_{23})g(r_{31})]$ of a simple liquid.

In Van Baal and Kikuchi's theory of liquids [16], the evaluation of cluster integrales where f-bonds are replaced by h-bonds such as

$$\Gamma(r_{12},r_{23},r_{31}) \equiv \int h(r_{12})h(r_{24})h(r_{34})d\mathbf{r}_4 \qquad (4.3)$$

where

$$h(r) \equiv g(r) - 1$$

is necessary, and their scheme involving the iteration with such terms as (4.3) requires much computer time. The knowledge of $\delta_1^{(3)}$ serves as a first approximation of (4.3) and gives an insight into the problem.

It has been reported that in supercooled and rapidly quenched states of simple liquids the three particle distribution function bears quite a different feature from that in the states above the triple point to reflet very strong triplet crrelations at extremely low temperature [17]. We have calculated $\delta_1^{(3)}$ of our model at lower temperature such as $kT/\varepsilon = 0.5$, i.e. $kT/u = 0.23$, which can be compared with the results by the molecular dynamics simulation of the rapidly quenched states of the Lennard-Jones liquid. Details will be reported eleswhere [18].

The authers acknowledge helpful discussions with Professor S. Inawashiro and Professor R. Kikuchi.

Appendix Some useful formulae

$$\gamma_0(t_1-t_2)=-2^{-3/2}\Gamma(3/2)\Sigma_{n=0}^{\infty}\frac{J_{3/2+n}(t_1)}{t_1^{3/2}}\frac{J_{3/2+n}(t_2)}{t_2^{3/2}}C_n^{3/2}(\cos\psi_{t_1-t_2}). \tag{A.1}$$

$$\exp(i\mathbf{t}.\mathbf{r})=(2\pi)^{1/2}\Sigma_{p=0}^{\infty}(\tfrac{1}{2}+p)i^p\frac{J_{1/2+p}(tr)}{(tr)^{1/2}}P_p(\cos\psi_{\mathbf{t}-\mathbf{r}}). \tag{A.2}$$

$$C_n^{3/2}(\cos\psi)=\Sigma'^{n}_{u=0}(2u+1)P_u(\cos\psi), \tag{A.3}$$

where the summation Σ' for u runs only over integers with the same parity with n.

$$\int P_u(\cos\psi_{t1-t2})P_p(\cos\psi_{t1-t3})d\Omega_{t1} = \delta_{up}(4\pi/(2u+1))P_p(\cos\psi_{t1-t3}). \quad (A.4)$$

$$J_{n+1/2}(z) = (2\pi z)^{-1/2}\left[e^{iz}\Sigma_{r=0}^{n} \frac{i^{r-n-1}(n+r)!}{r!(n-r)!(2z)^r} + e^{-iz}\Sigma_{r=0}^{n}\frac{(-i)^{r-n-1}(n+r)!}{r!(n-r)!(2z)^r}\right]. \quad (A.5)$$

$$P\int_{-i\infty}^{i\infty} \frac{1}{s^m}\exp(sa)\,ds = \mathrm{sgn}(a)\pi i\,\frac{a^{m-1}}{(m-1)!}. \quad (A.6)$$

References

1. H. J. Raveché, R.D. Mountain and W.B. Street,
1972 J. Chem. Phys. 57 4999.

2. M. Tanaka and Y. Fukui, 1975 Prog. Theor. Phys. 52 1547

3. J. E. Mayer and E. W. Montroll, 1941 J. Chem. Phys. 9 2.

4. E. Meeron, 1958 Phys. Fluids 1 139.

5. B. R. A.Nijboer and L. Van Hove, 1952 Phy.Rev. 85 777.

6. D. A. McQuarrie, 1964 J. Chem. Phys. 40 3455.

7. S. Katsura and K. Nishihara, 1969 J. Chem. Phys. 50 3579.

8. R. Abe, 1959 Prog. Theor. Phys. 21 421.

9. J. S. Rowlinson, 1963 Mol. Phys. 6 517.

10. M. J. D. Powell, 1964 Mol. Phys. 7 591.

11. T. Kihara, 1953 Rev. Mod. Phys. 25 831.

12. S. Katsura, 1959 Phys. Rev. 115 1417; 1960 118 1667.

13. S. Katsura and Y. Abe, 1963 J. Chem. Phys. 39 2068.

14. J. E. Kilpatrick and S. Katsura, 1966 J. Chem. Phys. 45 1866.

15. A. C. Hearn, REDUCE2 users manual, (University of Utah 1973)
W. S. Brown and A. C. Hearn, 1979 Ceruput. Phys. Commun. 17 2

16. C. M. Van Baal and R. Kikuchi, to be published.

17. M. Tanaka, 1983 J. Phys. Soc. Jpn. 52 1970, and 2046.

18. H. Satoh, M. Tanaka and S. Katsura, to be published.

Table 1. The value of $V(a,b,c;r_a, r_b, r_c)$. Other cases which are obtained by cyclic permutations of indices are omitted. The numbers [1] to [9] correspond to the configurations of three spheres shown in Fig.3.

$a>r_b+r_c$ or $b>r_c+r_a$ or $c>r_a+r_b$	[1] 0			
$a<r_b+r_c$ and $b<r_c+r_a$ and $c<r_a+r_b$	$Q \geq 0$	[2] $2V_t-2(Z_a+Z_b+Z_c)+2(Y_a+Y_b+Y_c)$		
	$Q < 0$	$I_a=I_b=I_c=0$	$L_a=1$ $L_b=L_c=0$	[3] Y_{a0}
			$L_a=0$ $L_b=L_c=1$	[4] $Y_{b0}+Y_{c0}-4\pi r_a^3/3$
			$L_a=L_b=L_c=1$	[5] 0
		$I_a=1$ $I_b=I_c=0$	[6] Y_{bo} $(r_b>r_c)$ Y_{c0} $(r_b<r_c)$	
		$I_a=0$ $I_b=I_c=1$	[7] $4\pi r_a^3/3$ $(2r_a<r_b+r_c+a)$	
			[8] Y_{a0} $(2r_a>r_b+r_c+a)$	
		$I_a=I_b=I_c=1$	[9] $4\pi r_m^3/3$ $r_m \equiv \min(r_a,r_b,r_c)$	

Figure captions

Fig.1 Geometry of intersections of three spheres centered at A, B, and C. The intersecting volumes V_t, Z_a and Y_a are given in (3.2), (3.3) and (3.4), respectively.

Fig.2 The distance F_a used in the indicator L_a.

Fig.3 Classification of intersection of three spheres. The numbers [1] to [9] correspond to each of the rows in Table 1.

Fig.4 The convergence of (2.8) in the analytic method for $\delta_1^{(3)}(r,r,r)$ at $kT/\epsilon = 2.0$. Solid line: geometrical method (exact), and Dotted lines: analytical method trancated at n = N in (2.8).

Fig.5 Schematic of the geometry in Figs.6 and 7. The distance r_{12} is fixed arbitarily and the dashed circles around the crosses denote the hard cores of the particles 1 and 2.

Fig.6 $\delta_1^{(3)}(r_{12},r_{23},r_{31})$ at $kT/\epsilon = 1.6$. (a): $r_{12} = 1.0$, (b): $r_{12} = 1.6$, (c): $r_{12} = 2.6$, (d) $r_{12} = 3.0$. $\delta_1^{(3)}$ vanishes outside the outmost dashed curve (see Table 1 [1], [5]).

Fig.7 $\delta_1^{(3)}(r_{12},r_{23},r_{31})$ at $kT/\epsilon = 5.0$. (a): $r_{12} = 1.0$, (b): $r_{12} = 1.6$, (c): $r_{12} = 2.6$, (d): $r_{12} = 3.0$.

Fig.8 General features of $\delta_1^{(3)}$ with varying r_{12} at lower

temperature. M and m denote the locations of local maximum and minimum, respectivly, and S the saddle point. $\delta_1^{(3)}$ is negative in the shaded region. (a): smaller r_{12}, (b): intermediate r_{12}, (c): larger r_{12}.

Fig.9 $\rho^{-1}\log\{g^{(3)}(r_{12},r_{23},r_{31})/[g(r_{12})g(r_{23})g(r_{31})]\}$ for the Lennard-Jones liquid at $\rho\sigma^3 = 0.850$ and $kT/u = 0.719$ with $r_{12} = 1.525\sigma$ [1]. $\delta_1^{(3)}$ is negative in the shaded region.

Fig.10 Comparison of the isosceles $\delta_1^{(3)}(s,r,r)$ at a fixed value of $s = 1.19$ with $\rho^{-1}\log\{g^{(3)}(s,r,r)/g(s)[g(r)]^2\}$ of Lennard-Jones liquid obtained by the molecular dynamics simulation: $kT/\varepsilon = 1.58$, $\rho = 0.64$. The value of s corresponds to the position of the first peak of g(r).

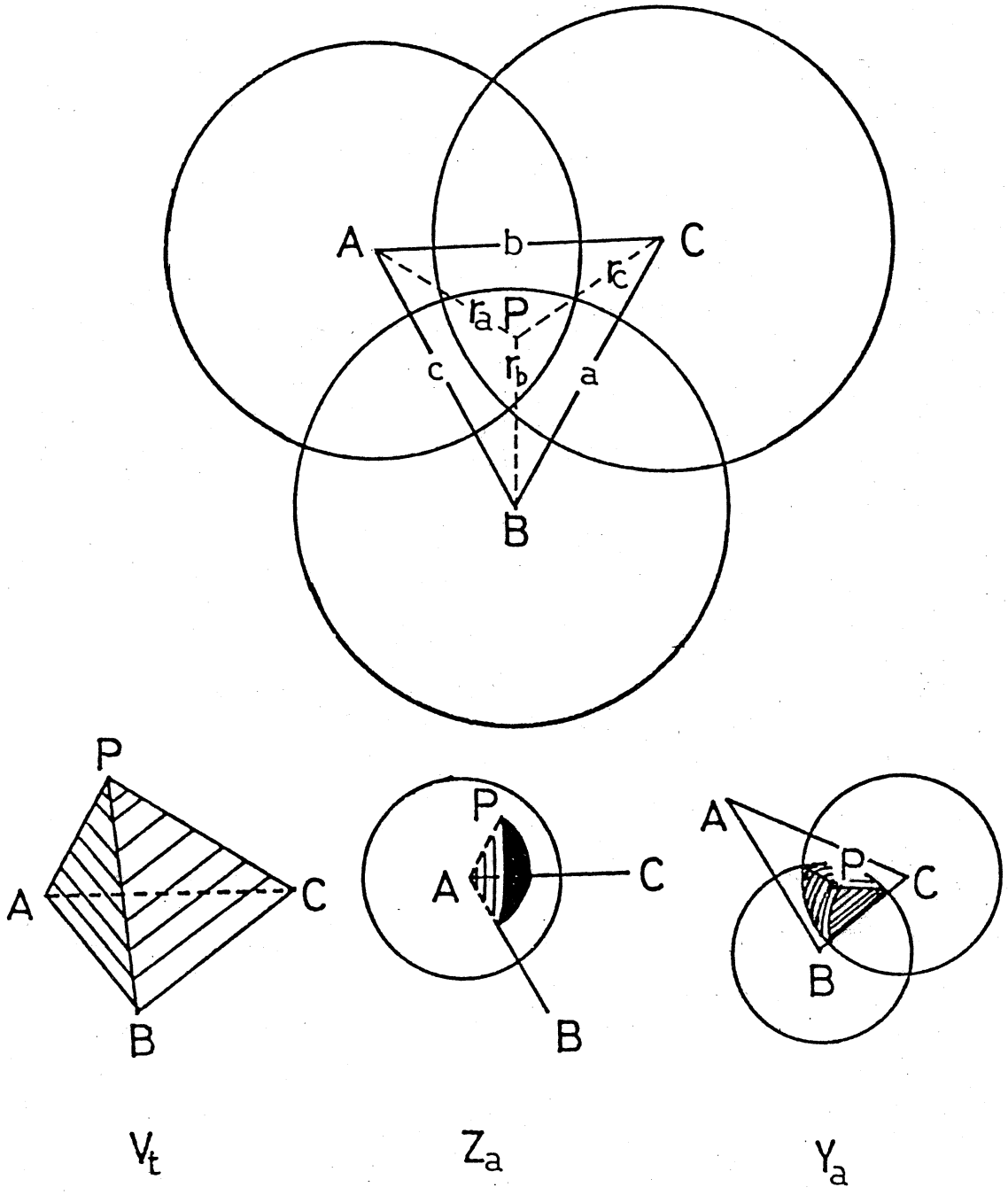

Fig.1

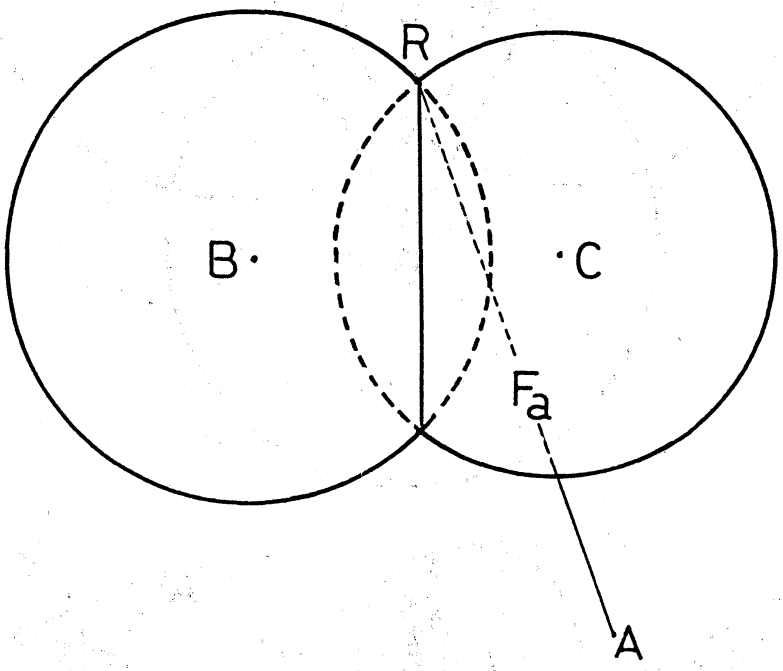

Fig.2

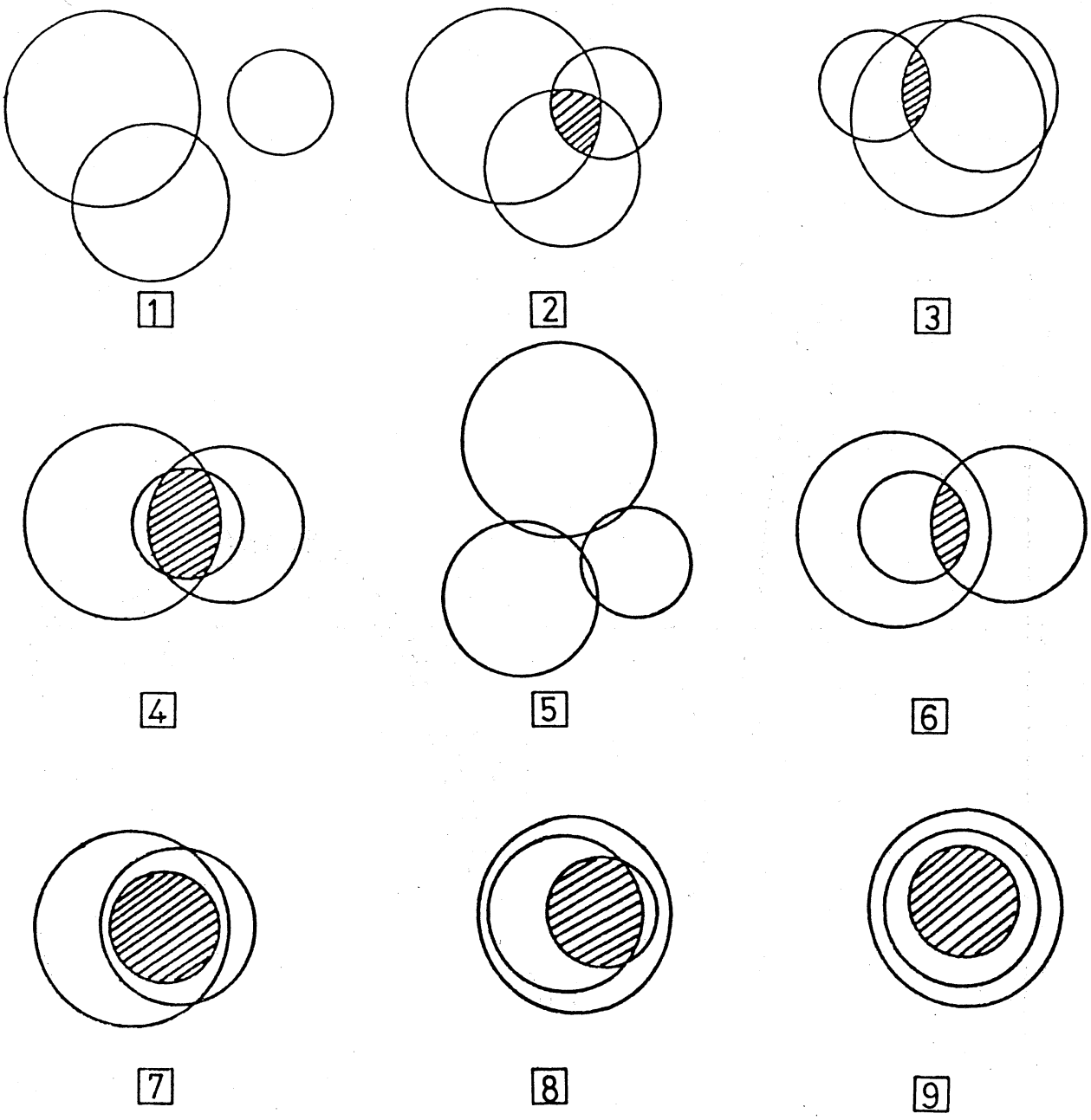

Fig.3

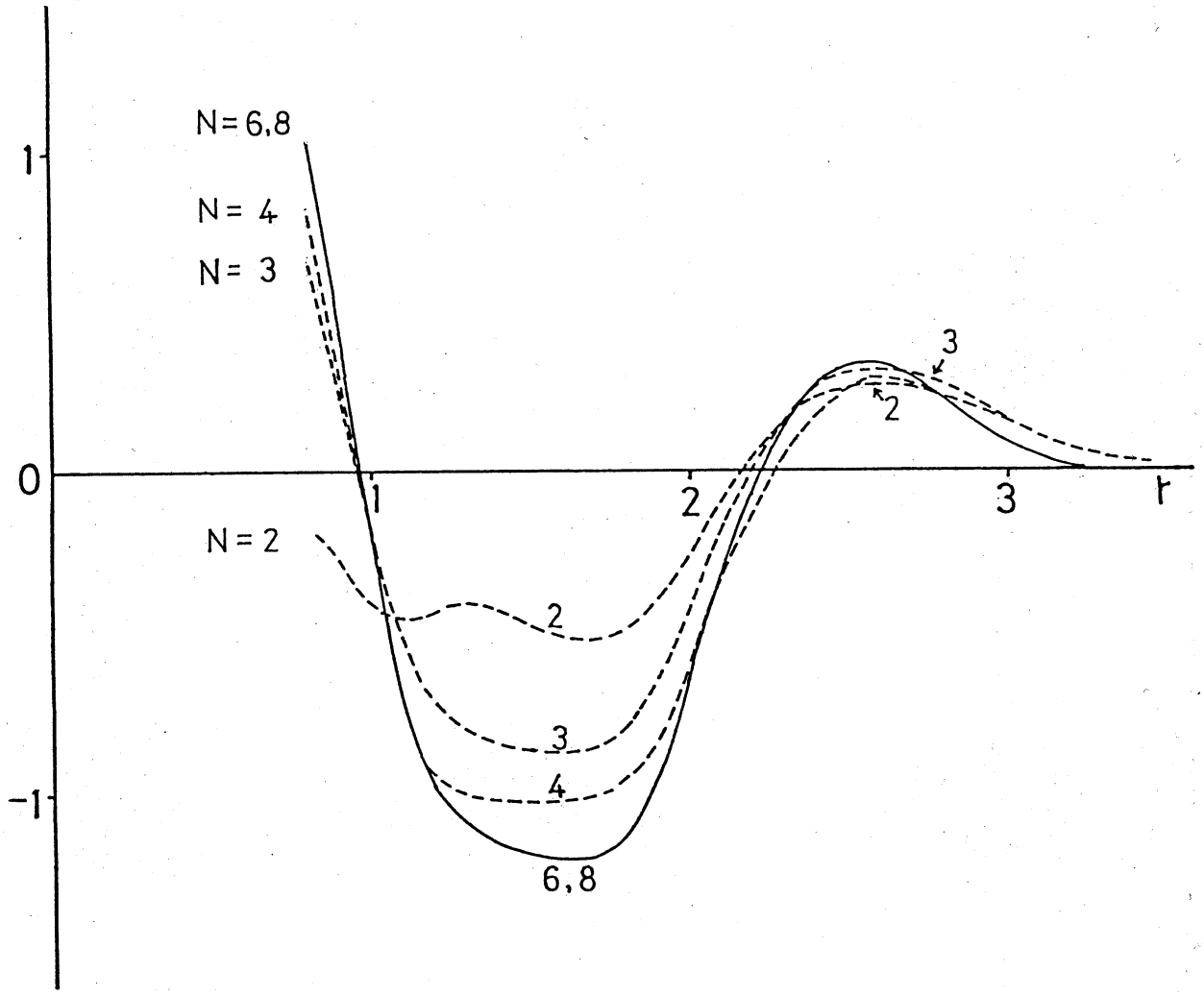

Fig.4

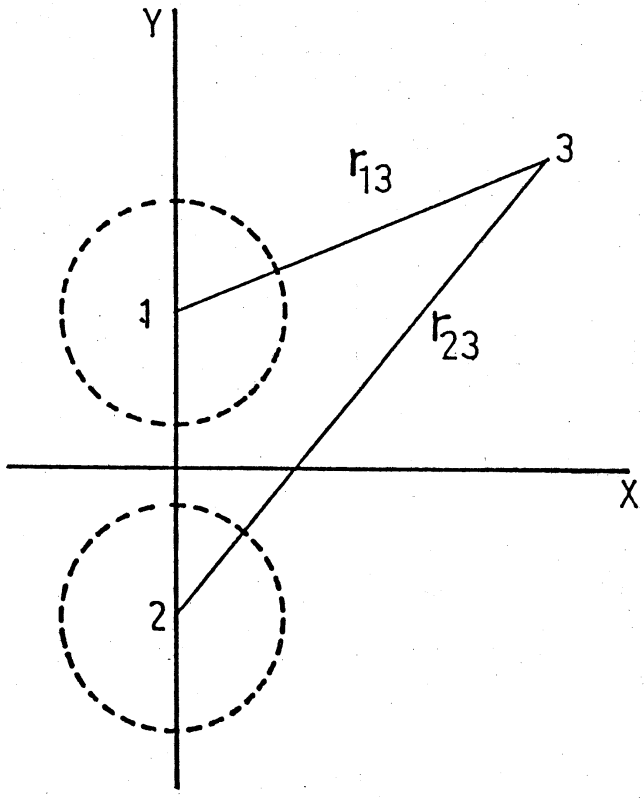

Fig.5

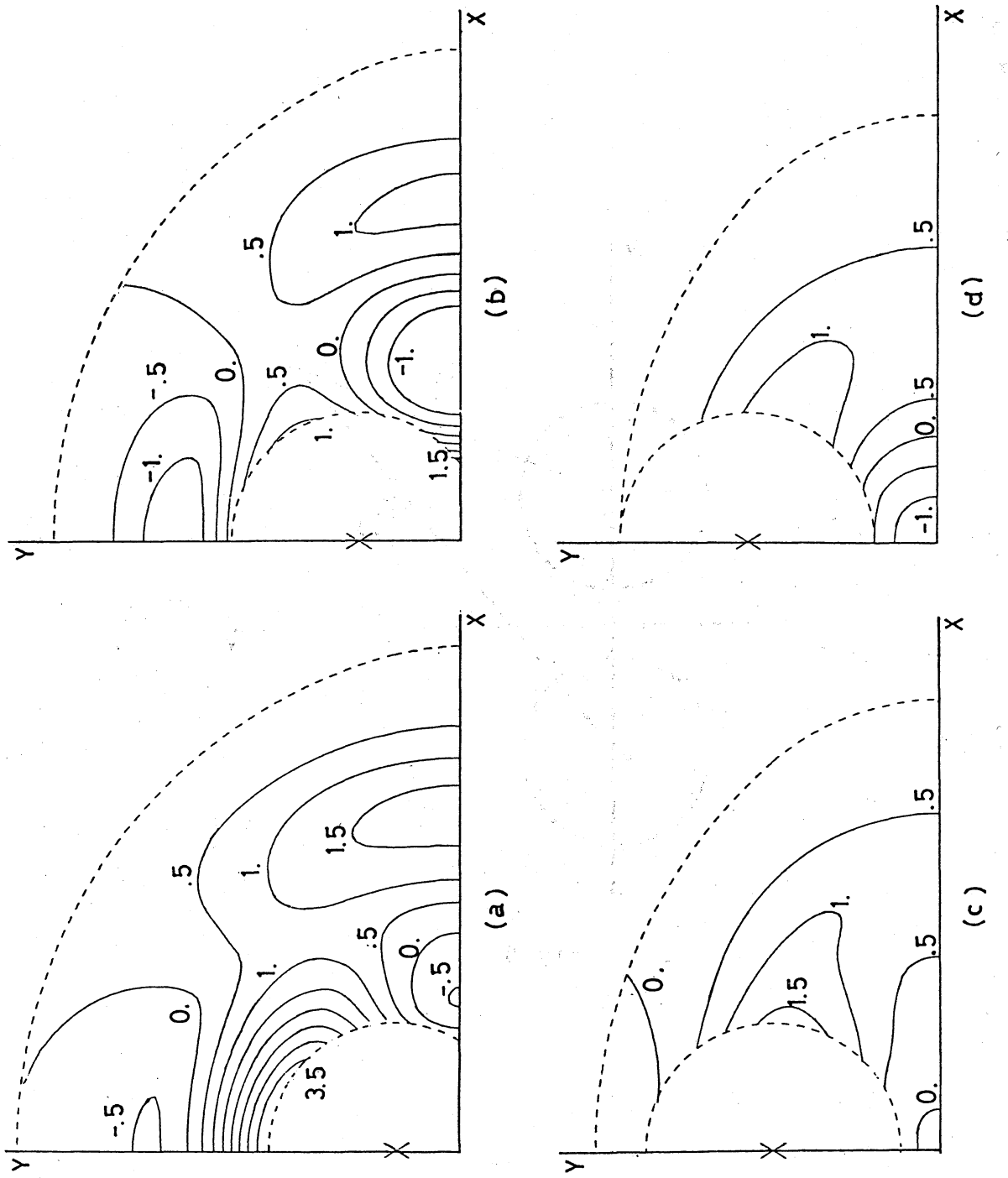

Fig.6

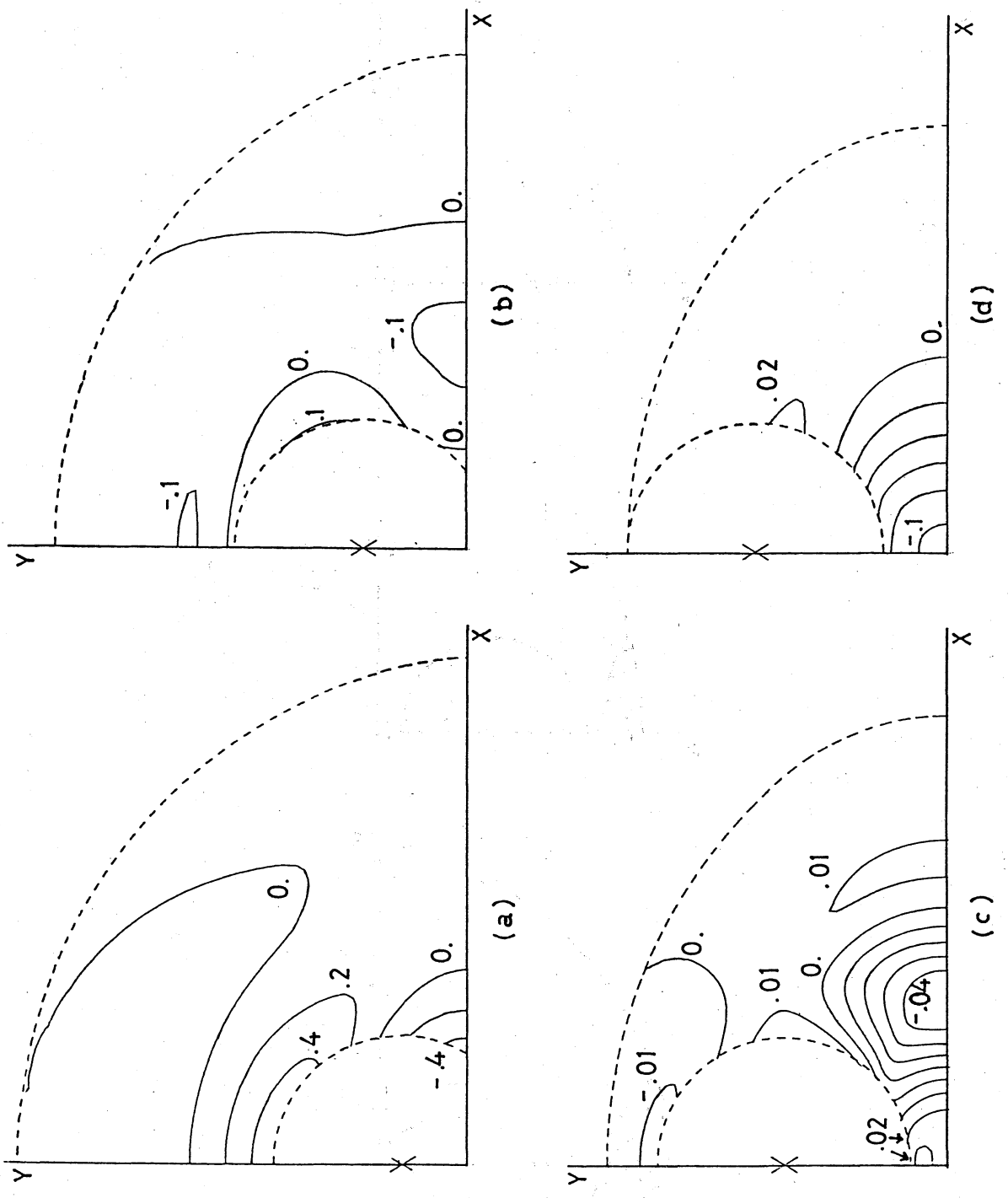

Fig.7

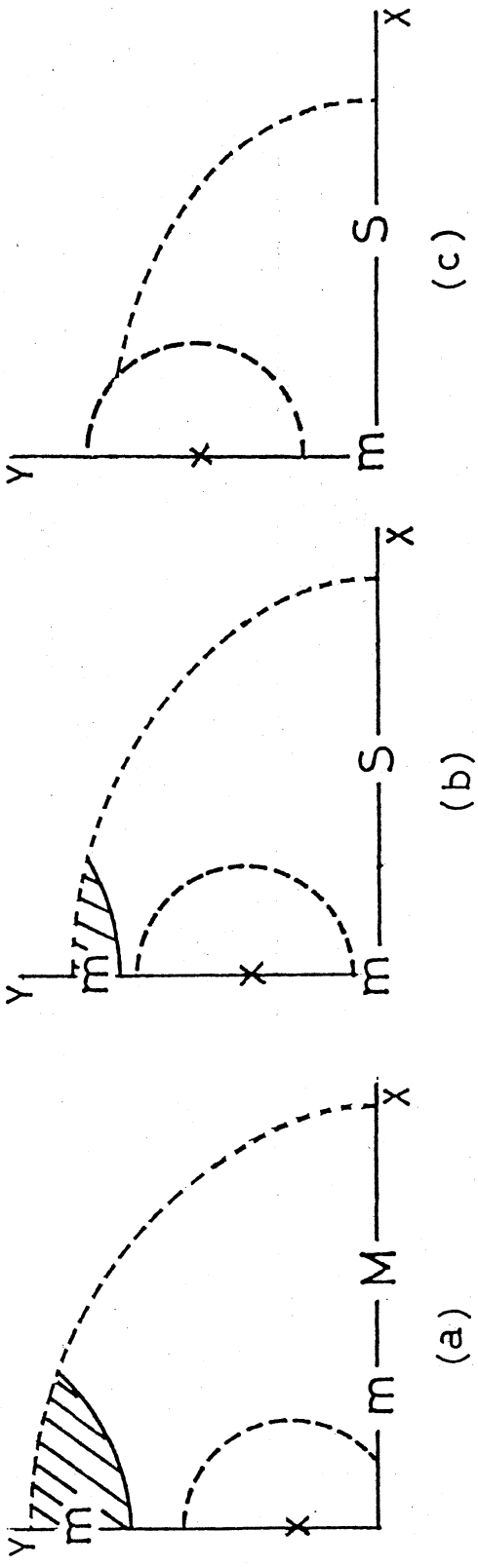

Fig.8

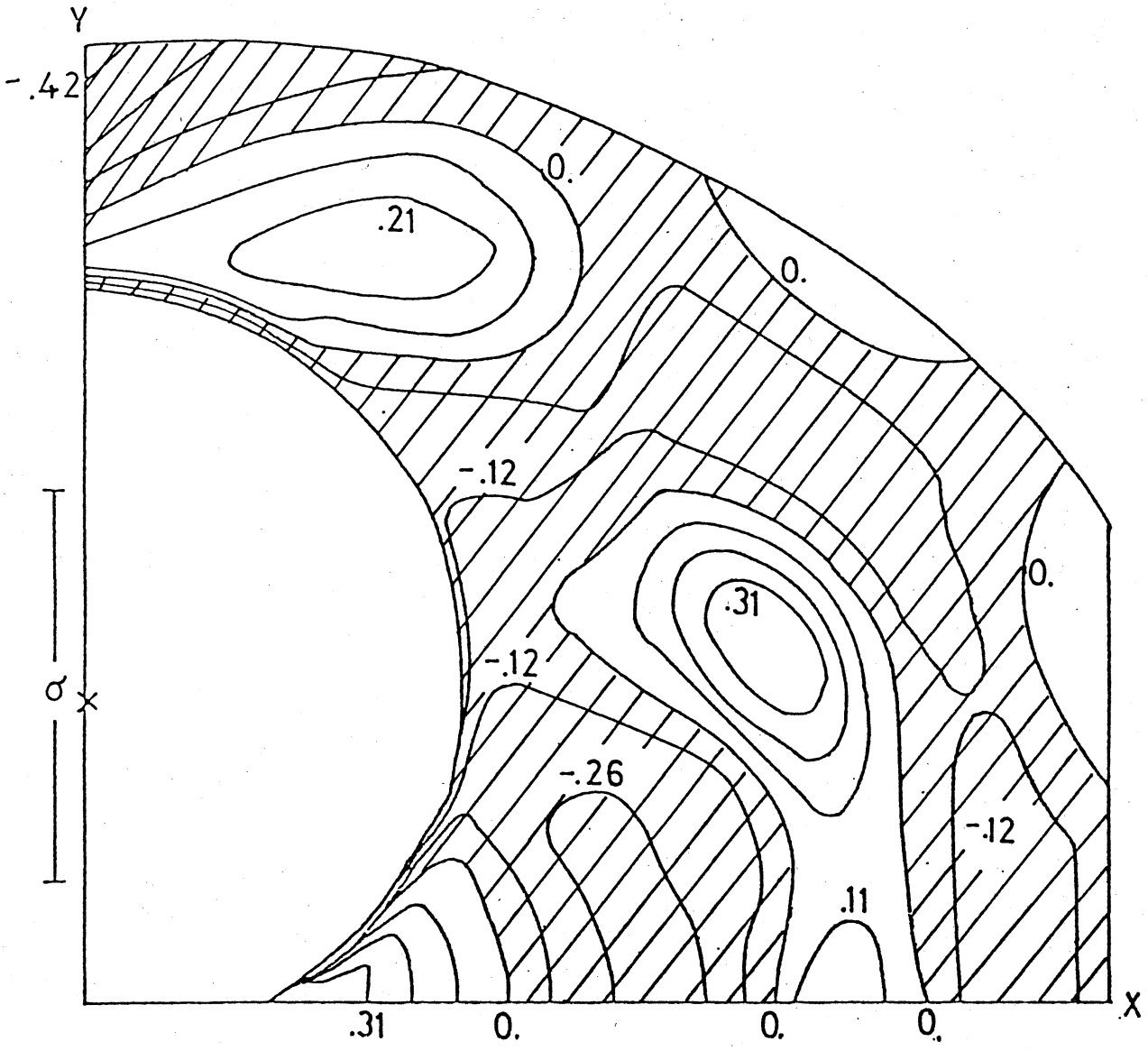

Fig.9

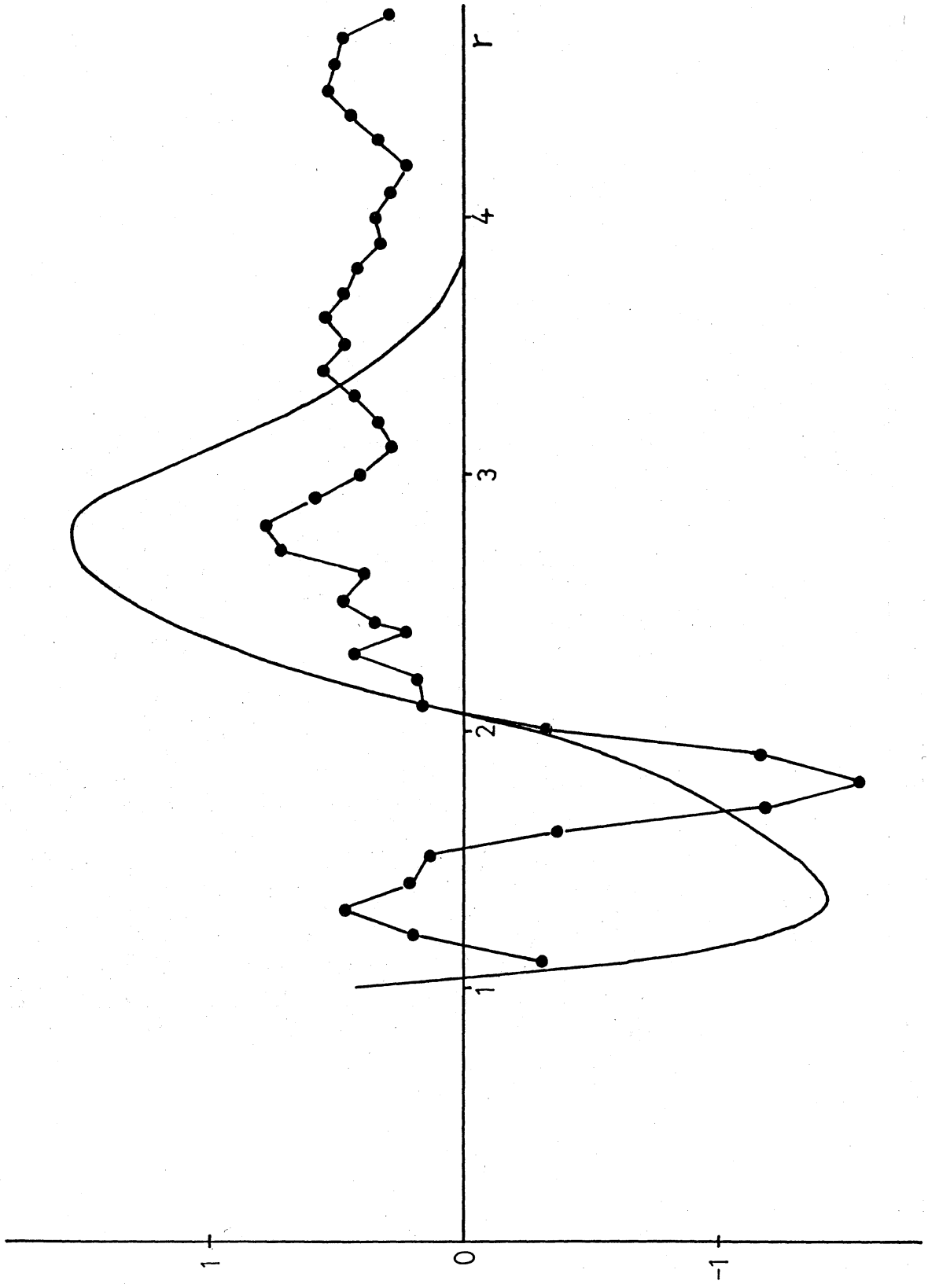

Fig.10